Biochemistry

Perspective

Cite This: Biochemistry 2019, 58, 4667−4676

pubs.acs.org/biochemistry

A Tour de Force on the Double Helix: Exploiting DNA Mechanics To Study DNA-Based Molecular Machines

Michael R. Wasserman and Shixin Liu*

Laboratory of Nanoscale Biophysics and Biochemistry, The Rockefeller University, New York, New York 10065, United States

ABSTRACT: DNA is both a fundamental building block of life and a fascinating natural polymer. The advent of single-molecule manipulation tools made it possible to exert controlled force on individual DNA molecules and measure their mechanical response. Such investigations elucidated the elastic properties of DNA and revealed its distinctive structural configurations across force regimes. In the meantime, a detailed understanding of DNA mechanics laid the groundwork for single-molecule studies of DNA-binding proteins and DNA-processing enzymes that bend, stretch, and twist DNA. These studies shed new light on the metabolism and transactions of nucleic acids, which constitute a major part of the cell's operating system. Furthermore, the marriage of single-molecule fluorescence visualization and force manipulation has enabled researchers to directly correlate the applied tension to changes in the DNA structure and the behavior of DNA-templated complexes. Overall, experimental exploitation of DNA mechanics has been and will continue to be a unique and powerful strategy for understanding how molecular machineries recognize and modify the physical state of DNA to accomplish their biological functions.

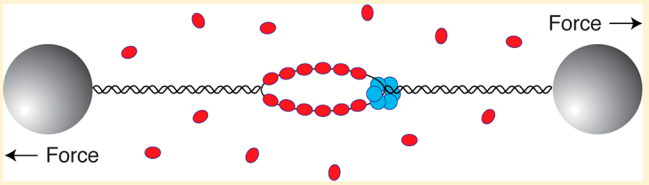

The DNA double helix is arguably the most celebrated discovery in biology during the past century.[1−3] In the ensuing decades, individual DNA molecules were directly visualized under electron and fluorescence microscopes.[4−7] During the past 25 years, the development of single-molecule manipulation methods has led to elucidation of the mechanical properties of DNA (reviewed in refs 8 and 9). Single-molecule methods circumvent the need for synchronization and allow for real-time observation. These tools, initially used to observe and manipulate DNA, have also been employed to dissect the molecular mechanisms of DNA-binding proteins and DNA-processing enzymes (reviewed in refs 10 and 11). In this Perspective, we will first review how single-molecule force spectroscopy has enabled detailed investigation of the elastic properties of DNA. We will then discuss how the knowledge of DNA mechanics has facilitated the studies of DNA-based biological processes such as DNA packaging and replication. Finally, we will discuss how recent development in combined fluorescence and force microscopy has allowed direct correlation between DNA structure and mechanics.

DNA MECHANICS

DNA has several unique properties as a polymer. Its extensive hydrogen bonding and base stacking render it highly stiff; the negative charge on every backbone phosphate also makes it one of the most charged polymers known in nature. Characterization of the elastic properties of DNA was greatly facilitated by the development of single-molecule force manipulation methods, which exert controlled force on a biomolecule and precisely measure its mechanical response.[12] The viscoelastic properties of DNA have been investigated by magnetic tweezers,[13,14] micro fibers,[15] hydrodynamic flow,[16] and optical tweezers (Figure 1A).[17] The force−extension (F−x) behavior of double-stranded DNA (dsDNA) can be described well by a worm-like-chain (WLC) model (Figure 1B):

$$F = \frac{k_B T}{L_p}\left[\frac{1}{4\left(1-\frac{x}{L_0}\right)^2} - \frac{1}{4} + \frac{x}{L_0}\right]$$

where F is the applied force, x is the DNA extension, k_B is the Boltzmann constant, T is the absolute temperature, and L_0 is the DNA contour length (maximum end-to-end distance).[18] The WLC model employs a coarse-grained treatment on DNA, ignoring local variations in sequence and helical structure, and characterizes the flexibility of the polymer with a single parameter, the persistence length (L_p). L_p can be intuitively understood as the length scale over which the direction of the polymer chain persists under thermal fluctuations. In a typical physiological buffer, L_p for dsDNA is ∼50 nm or ∼150 bp and has been shown to depend on the ionic strength and valency.[19,20] However, DNA exhibits surprisingly high bendability at short length scales (<100 bp).[21] This extreme flexibility can be described by modified WLC models that allow for the formation of transient kinks or bubbles.[22,23] Moreover, a "twistable" WLC model was proposed[24] to account for the response of the helical structure of DNA to torsional tensions.[25,26]

Special Issue: Mechanical Forces in Biochemistry

Received: April 17, 2019
Revised: June 18, 2019
Published: June 28, 2019

DOI: 10.1021/acs.biochem.9b00346
Biochemistry 2019, 58, 4667−4676

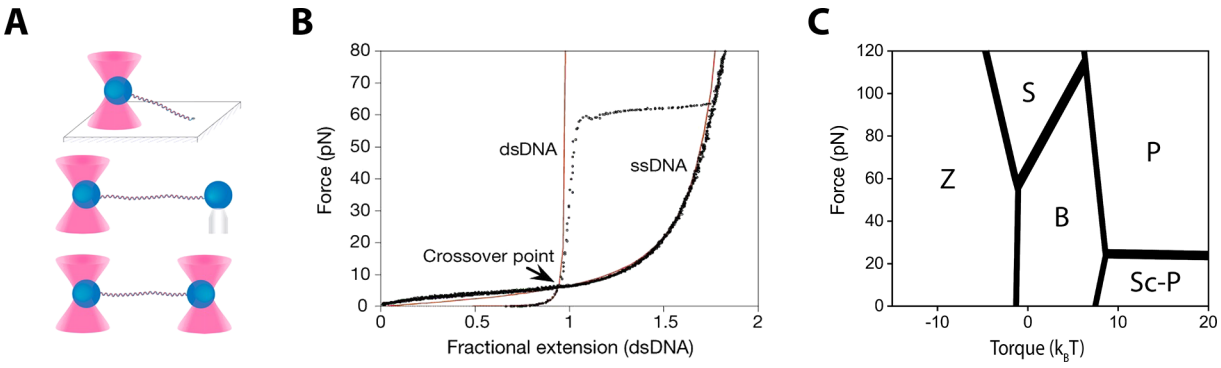

Figure 1. Single-molecule manipulation to elucidate DNA mechanics. (A) Force measurements of single DNA molecules are enabled via multiple optical-trapping geometries, in which one end of the DNA is tethered to an optically trapped micrometer-sized bead and the other end is tethered to a microscope slide surface (top), a micropipette-suctioned bead (middle), or another optically trapped bead (bottom). Panel A reprinted with permission from ref 27. Copyright 2014 American Chemical Society. (B) Force–extension behavior of ssDNA and dsDNA. The red lines indicate the WLC model prediction. At forces above the crossover point (~6 pN), ssDNA is longer than dsDNA. Panel B reproduced with permission from ref 28. Copyright 2000 Springer Nature Publishing AG. (C) Force–torque phase diagram of dsDNA. Note that along the borders between regions, adjacent phases coexist in equilibrium: Z, Z-DNA; S, S-DNA; B, B-DNA; P, P-DNA (extended and overtwisted); Sc-P, plectonemically supercoiled DNA. Panel C adapted with permission from ref 29. Copyright 2001 American Physical Society.

A flexible polymer tends to coil randomly in solution, resulting in an end-to-end distance much shorter than its contour length. Thus, pulling a flexible chain into an extended one is entropically unfavorable. A tension of ~6 pN, a typical amount of force exerted by biomolecular motors, is needed to stretch dsDNA to 95% of its contour length (Figure 1B). In comparison, single-stranded DNA (ssDNA) has a much shorter persistence length (on the order of 1 nm) and is more contractile, adopting conformations more compact than those of dsDNA at low forces.[30] At higher forces, the extension of ssDNA exceeds that of dsDNA and reaches nearly twice as long as dsDNA at full extension (Figure 1B).

DNA predominantly exists in a right-handed B-form in aqueous solution but can adopt a shorter and wider A-form structure under dehydrating conditions. Moreover, DNA with specific sequences can assume a left-handed Z form.[31] Besides these three well-known biologically active forms, single-molecule pulling experiments have revealed additional forms of DNA under specific force regimes. In particular, when the applied tension was increased to ~65 pN, B-DNA was found to undergo a transition to an extended form that is ~70% longer.[15,17] There has been considerable debate regarding whether this overstretched form of dsDNA represents a new base-paired structure (coined the term "S-DNA") or comprises two denatured ssDNAs.[32,33] Recent studies showed that both mechanisms can be simultaneously at work. Force-induced denaturation is favored when the AT content in the DNA is high; while for GC-rich sequences, the DNA undergoes a reversible overstretching transition into an elongated, underwound, yet base-paired form, supporting the existence of S-DNA.[34,35]

Besides tension-induced structural transitions, torque can also cause DNA to adopt distinct conformations.[36] For torsionally constrained DNA (via multiple points of attachment to the bead at each terminus), an overwound structure with the backbones tightly wrapped around and the base pairs flipped out, known as P-DNA, was observed when the DNA overstretched at forces of >110 pN.[37] The twist elasticity of DNA has been extensively reviewed elsewhere.[38,39] Through a combination of experimental manipulation and statistical–mechanical modeling, the force–torque phase diagrams for DNA have been depicted (Figure 1C).[29,40]

The well-characterized elasticity combined with its ease of construction makes DNA a popular choice as a molecular handle[41] for single-molecule studies of protein/RNA folding[42,43] and biomolecular motors.[44] More recently, researchers have utilized DNA origami technology to construct bundled DNA beams that are much more rigid than conventional dsDNA for ultra-high-resolution measurements.[45,46]

EXPLOIT DNA MECHANICS TO STUDY BIOLOGY

DNA is under constant tension inside the cell: It is wrapped around histones,[47] unwound by helicases,[48] and twisted and untwisted by RNA polymerases[49] and topoisomerases,[50] to name a few examples. The elucidation of the mechanical properties of DNA has greatly facilitated the study of molecular machines that act on DNA, yielding mechanistic insights into their force-generation mechanisms and the coordination of their components.[51] Below we use two example systems to demonstrate how the knowledge of DNA elasticity has inspired creative assays for studying biological processes.

Viral DNA Packaging. The exact derivation of DNA extension as a function of force makes it possible to convert movement in distance into changes in base pairs, thereby providing exquisite insight into the operating mechanism of protein machineries that translocate on DNA, such as RNA polymerases[52] and viral DNA packaging motors.[53] In the latter case, dsDNA genomes are pumped into preformed protein capsids during viral assembly. The ring-shaped packaging motors are among the most powerful molecular machines found in nature. To compact the stiff, highly charged dsDNA to near-crystalline densities into a small capsid, the packaging motor needs to generate a large amount of force, up to 60 pN, to overcome major energetic barriers. The packaging motor of bacteriophage φ29, one of the best-characterized molecular machines thus far, is a homopentameric ring ATPase that packs a 19.3 kb genome into a capsid 50 nm in height and 40 nm in diameter.[54] Using a dual-trap optical tweezers instrument, the Bustamante group was able to detect discrete DNA translocation cycles of the ring motor (Figure 2A). Under low external forces (<10 pN), DNA is translocated in 10 bp cycles, each consisting of an ATP-binding dwell phase and a DNA-translocating burst phase (Figure 2B). Under high

DOI: 10.1021/acs.biochem.9b00346
Biochemistry 2019, 58, 4667–4676

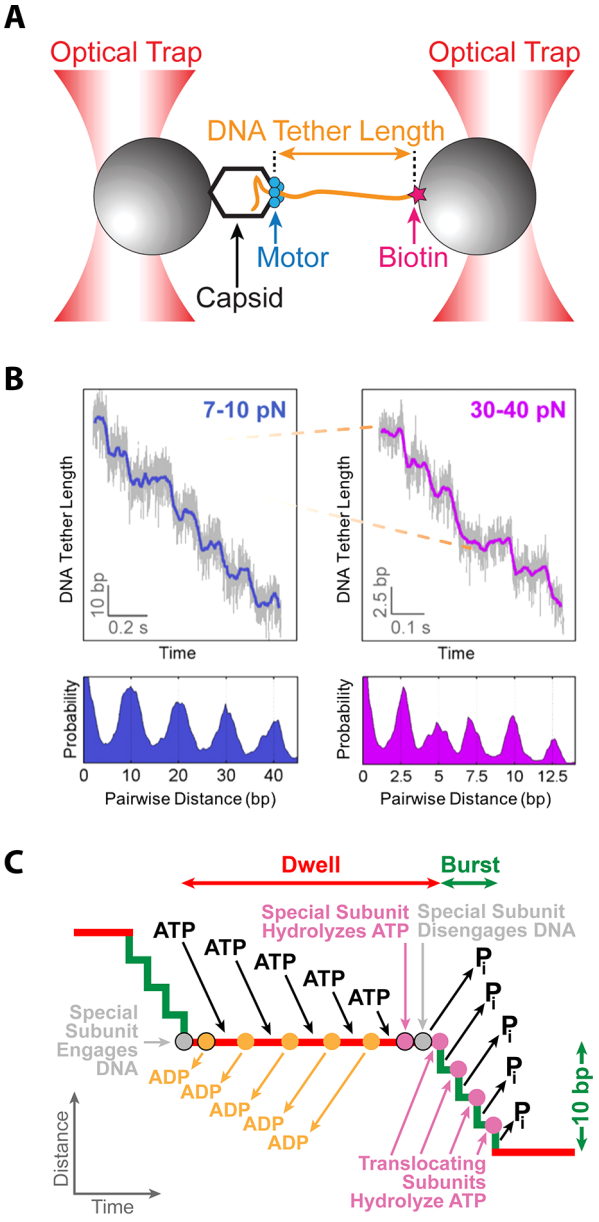

Figure 2. Optical-trapping assay to study viral DNA packaging. (A) Schematic of a dual-trap optical tweezers assay to study DNA translocation by the bacteriophage φ29 packaging motor. Panel A reproduced with permission from ref 58. Copyright 2014 Elsevier. (B) Representative packaging traces (top) collected at low (left) and high (right) forces. At high forces, the 10 bp bursts seen at low forces are decelerated enough to reveal 2.5 bp steps. Pairwise distance analysis (bottom) for the corresponding traces. Panel B reproduced with permission from ref 56. Copyright 2012 Elsevier. (C) Mechanochemical model for the φ29 packaging motor showing DNA translocation cycles with a dwell-burst structure. Panel C adapted with permission from ref 58. Copyright 2014 Elsevier.

external forces (30−40 pN), each 10 bp burst is decelerated and can be shown to be composed of four 2.5 bp steps. Each step is powered by the release of an inorganic phosphate molecule produced by ATP hydrolysis. Subsequent experiments using nucleotide analogues and ATPase mutants mapped specific chemical transitions (such as ATP hydrolysis and ADP release) onto the dwell-burst pathway, revealing intricate, clocklike coordination among the five ring subunits (Figure 2C).[55−57]

The non-integer 2.5 bp step size is surprising. This result argues against any mechanism in which every motor subunit makes identical chemical contacts with the DNA during translocation. It further suggests that only four of the five subunits participate in DNA translocation per cycle. Indeed, it was shown that the translocating subunits make nonspecific contacts with the DNA during the burst phase[59] and that the ring symmetry is broken through specific electrostatic interaction with DNA backbone phosphates, bestowing a special regulatory role upon the contacting subunit.[56,57]

It was proposed[60] and experimentally observed[61] that DNA inside the capsid is organized into a spool, which may require rotation of the DNA to relieve the torsional strain. In addition, the small difference between the 10.0 bp burst size of the motor and the 10.4 bp helical pitch of B-form DNA entails that the DNA may need to rotate relative to the motor to make crucial electrostatic contacts at the beginning of each cycle. To directly probe DNA rotation during translocation, a third "rotor bead" was introduced to the standard two-bead optical tweezers assay, which allowed angular changes in the DNA around its helical axis to be monitored concomitantly with its linear translocation.[58] A similar setup was previously used to measure the twist elasticity of DNA.[62] The DNA was shown to rotate on average by ∼1.5°/bp in a left-handed direction. Thus, the packaging motor can simultaneously generate force and torque, both of which can reach values high enough to denature DNA. The quantitation of DNA rotation also suggests that the same subunit makes the specific DNA interactions cycle after cycle, thus significantly constraining the possible models for the identity of the special subunit. After a 10 bp burst, the DNA backbone winds by 346°. Thus, a 14° rotation is required to realign the DNA with the subunit that makes contacts in the previous cycle, thereby yielding an average rotation density of 1.4°/bp.

DNA packaging has long been anticipated to slow as DNA fills up the capsid due to the mounting internal pressure working against the motor. This was directly proven by the single-molecule packaging assay showing that the velocity of the φ29 packaging motor decreases from an initial value of >100 bp/s to essentially zero when the entire genome length is internalized.[63] Subsequent high-resolution measurements revealed that the internal pressure affects multiple aspects of the mechanochemical cycle of the motor, including slowing ATP binding during the dwell phase and DNA translocation during the burst phase.[58] These results led to an estimation of the final internal pressure to be ∼20 atm, a remarkably large number that is consistent with predictions from analytical modeling and numerical simulation studies.[64−66] Furthermore, the φ29 packaging motor was observed to take smaller bursts per cycle (10 bp at low filling vs 9 bp at high filling) and smaller elementary steps (2.5 bp at low filling vs 2.3 bp at high filling). An accompanying change in the DNA rotation density was also observed (∼1.5°/bp at low filling vs ∼5°/bp at high filling). These concerted adjustments ensure that the distinct functions and coordination of the ring subunits are preserved even in the face of drastically different operating conditions.[58] In addition, a recent simulation study suggested that, instead of being a passive substrate, the DNA itself is an active component of the packaging machinery, driving its own translocation by undergoing cyclic conformational distortions inside the viral portal channel.[67] Overall, this model system showcases how knowledge in DNA mechanics allows for a

DOI: 10.1021/acs.biochem.9b00346
Biochemistry 2019, 58, 4667−4676

detailed mechanistic dissection of the three-dimensional trajectories of molecular machines that track on DNA.

DNA Replication. Many DNA-based cellular processes involve interconversion between dsDNA and ssDNA. The DNA duplex is unzipped into two separate strands by a multitude of helicases or degraded into ssDNA by exonucleases. On the other hand, DNA polymerases copy ssDNA templates into duplexes. The differential elasticity between ssDNA and dsDNA has been exploited to follow the progression of these biochemical reactions in real time without having to fluorescently label the enzymes. This was first used to study bacteriophage T7 DNA polymerase by optical tweezers[28] and magnetic tweezers.[68] Interestingly, it was found that at high forces (>40 pN), the nucleolytic activity of the polymerase is greatly stimulated, effectively converting the polymerase into an exonuclease.[28] Moreover, monitoring the enzymatic behavior as a function of applied tension unveiled intermediate states in the kinetic pathway that are related to the proofreading activity of the polymerase.[69]

van Oijen and co-workers developed a single-molecule DNA flow-stretching assay that can monitor many molecules at the same time, thus affording a throughput that is larger than that of the optical tweezers assay. In this setup, bacteriophage λ genomic DNA is anchored to a coverslip surface on one end and conjugated to a micrometer-sized bead on the other end. The DNA is then stretched by a hydrodynamic flow (Figure 3A). This setup was first utilized to study the activity of phage λ exonuclease, which converts dsDNA into ssDNA.[70] Later, this setup was applied to the phage T7 DNA replication system.[71] Here a bead is attached to the parental end of a forked DNA substrate. At a typical stretching force of ~2 pN, ssDNA is much shorter than dsDNA (Figure 1B). Leading-strand synthesis results in a shortening of the tether length due to accumulation of the lagging-strand ssDNA (Figure 3B). In the presence of lagging-strand synthesis, gradual shortening of the DNA followed by sudden lengthening was observed, which was interpreted as formation and subsequent fast release of replication loops in the lagging strand. These looping events were also observed in single-molecule FRET[72] and magnetic tweezers assays.[73] Further analysis of the loop sizes and lag times between loops suggested that the initiation of primer synthesis ("signaling" mechanism) and the encounter with a downstream Okazaki fragment ("collision" mechanism) can both serve as a trigger for loop release. Such a dual-trigger mechanism ensures the timely reset of the enzymatic apparatus at the replication fork after the completion of each round of Okazaki fragment synthesis.[74] Thus, this simple and elegant assay, chiefly utilizing DNA elasticity, yielded key insights into the coordination between continuous leading-strand synthesis and discontinuous lagging-strand synthesis.

The same group later developed a more sophisticated assay to simultaneously follow T7 leading-strand synthesis and lagging-strand loop formation by attaching two beads to two arms of the forked DNA.[77] This assay revealed that the looping events in the lagging strand contain both ssDNA loops formed during priming (priming loop, more frequent) and ss−ds ones that support Okazaki fragment synthesis (replication loop, less frequent). This study also showed that lagging-strand polymerases are often released from the replisome to complete Okazaki fragment synthesis behind the fork. These results depict a highly plastic replisome that can access multiple reaction pathways to achieve efficient and robust replication.

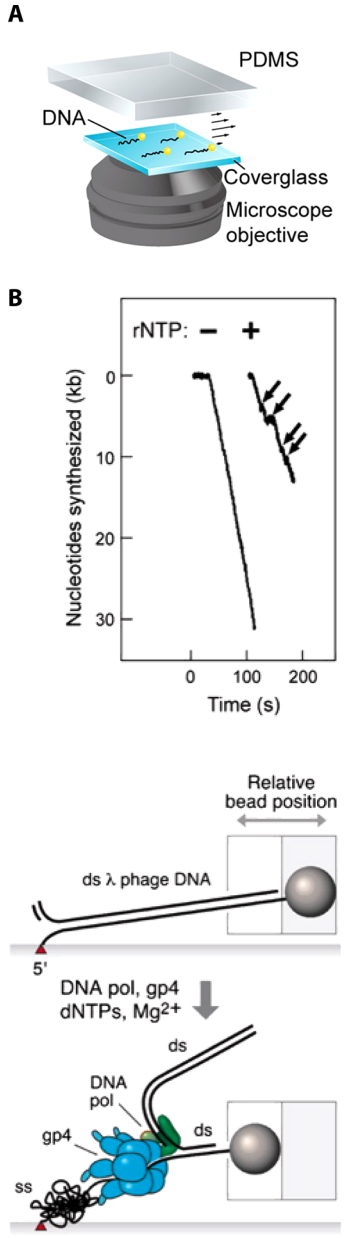

Figure 3. Flow-stretching assay to study DNA replication. (A) Schematic of a DNA flow-stretching assay. Individual DNA molecules are tethered to the surface of a flow cell on one end and conjugated to a bead on the other end. Panel A reproduced with permission from ref 75. Copyright 2017 National Academy of Sciences. (B) Representative single-molecule trajectories (top) with and without ribonucleotides required for lagging-strand priming. Arrows indicate pausing events. Schematic (bottom) depicting that leading-strand synthesis causes conversion of the 5′ tail of the tethered strand from dsDNA to ssDNA, resulting in a decrease in the tether length. Panel B reproduced with permission from ref 76. Copyright 2007 Wiley. Panel B originally adapted with permission from ref 71. Copyright 2006 Springer Nature Publishing AG.

The DNA flow-stretching assay has also been applied to the *Escherichia coli* replisome to investigate the processivity of the DNA polymerase III holoenzyme and its regulation by the DnaB helicase and DnaG primase.[78] More recently, it was demonstrated in a eukaryotic system from *Saccharomyces cerevisiae*,[75] which utilizes dedicated leading- and lagging-strand polymerases and more regulatory factors. Meanwhile, a

DOI: 10.1021/acs.biochem.9b00346
Biochemistry 2019, 58, 4667−4676

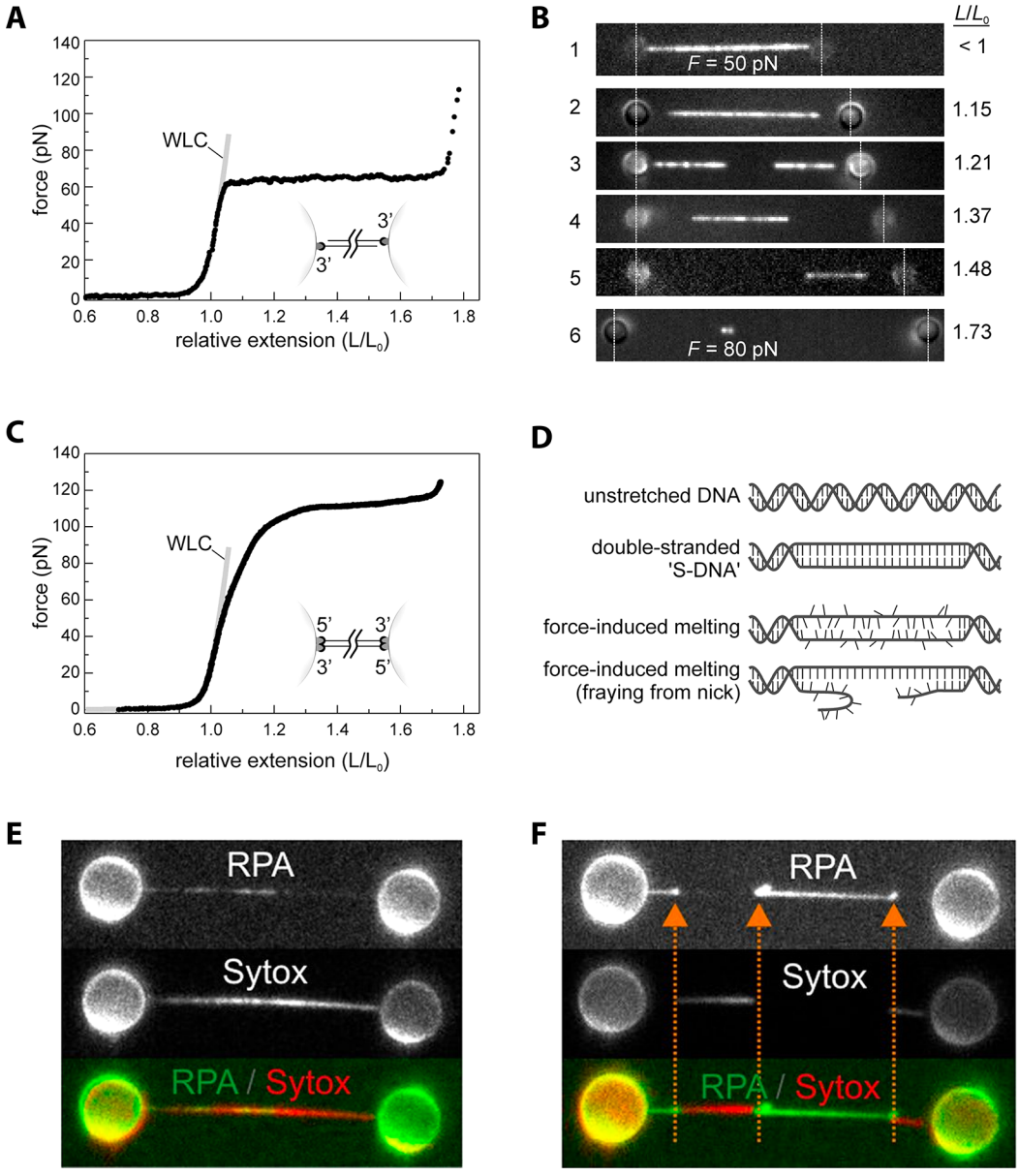

Figure 4. DNA structural transitions revealed by combined fluorescence–force microscopy. (A) Representative force–extension curve for dsDNA tethered to optically trapped beads via the 3′ end of each strand. (B) Fluorescence images of a dsDNA molecule tethered by the geometry depicted in panel A and stained with the intercalating dye YOYO. At tensions resulting in tether lengths greater than the contour length (L_0), unstained regions emerged, signifying the overstretching transition. (C) Representative force–extension curve for dsDNA tethered to beads via both ends of each strand. Here the overstretching transition occurs at ~110 pN. (D) Cartoon representations of various structural forms when dsDNA is overstretched. (E) Fluorescence images of an overstretched DNA that is topologically closed but torsionally relaxed. At low ionic strengths, melting bubbles are visualized with fluorescent RPA. dsDNA regions are indicated by the intercalating dye Sytox. (F) Fluorescence images of an overstretched and nicked DNA. Here strand unpeeling is favored, as indicated by the orange arrows. Panels A–D reproduced with permission from ref 33. Copyright 2009 National Academy of Sciences. Panels E and F reproduced with permission from ref 90. Copyright 2013 National Academy of Sciences.

number of other single-molecule assays based on fluorescence imaging of stretched DNA (for example, rolling circle and DNA curtains) have also been developed to study various aspects of DNA replication, such as initiation, lesion bypass, and polymerase exchange.[79−82]

CORRELATIVE INTERROGATION OF DNA STRUCTURE AND MECHANICS

The combination of single-molecule fluorescence spectroscopy and force spectroscopy allows multiplexed measurements of DNA conformation and protein–DNA interaction.[83−87] Such interrogation has enabled direct correlation between the force applied to DNA and the structural transitions that it undergoes and has yielded key information about the stoichiometry, dynamics, and force dependence of DNA-templated molecular assemblies.

Force-Induced Conversion between dsDNA and ssDNA. Using a single-molecule instrument that combines confocal fluorescence microscopy, dual-trap optical tweezers, and automated microfluidics, Wuite, Peterman, and co-workers directly visualized the structural transitions of DNA during overstretching.[33] They used the intercalating dye YOYO to

DOI: 10.1021/acs.biochem.9b00346
Biochemistry 2019, 58, 4667−4676

stain dsDNA that was linked to optically trapped beads via the 3′ end of each strand (Figure 4A). While the dsDNA molecule was stained along its full length under low forces, unstained segments appeared and grew when the tension was increased above 65 pN (Figure 4B). These segments were preferentially initiated from free DNA ends and internal nicks. To test whether these segments correspond to ssDNA regions, the authors then used fluorescently labeled ssDNA-binding protein (SSB), which wraps around ssDNA.[88] SSB foci were observed at edges of YOYO-labeled dsDNA segments and became brighter as the force increased. These results were interpreted as SSB binding to relaxed ssDNA unpeeled from free ends and nicks. To study overstretching of DNA without preferred nucleation sites, the authors also designed DNA substrates that were linked to beads via both ends of each strand to prevent peeling from free ends (Figure 4C). Notably, these torsionally constrained constructs displayed an overstretching plateau at much higher forces (~110 pN), in agreement with an earlier report.[89] Single-stranded regions were generated above 110 pN, as indicated by the binding of RPA, another ssDNA-binding protein that can bind to ssDNA under tension (unlike SSB). This observation can be interpreted as the formation of single-stranded "melting bubbles". Overall, these results demonstrated force-induced melting of dsDNA into ssDNA during overstretching regardless of the DNA attachment geometry.

In a follow-up study,[90] the same group focused on the competition between three processes during overstretching: strand unpeeling, localized base-pair breaking (melting bubbles), and S-DNA formation (strand unwinding with base pairing maintained) (Figure 4D). The authors found that all three mechanisms are at work. In topologically closed but torsionally relaxed DNA where free ends and nicks are lacking, melting bubbles form preferentially in AT-rich regions at low ionic strengths (Figure 4E). The same type of construct was also used by another group to show that strand unpeeling is not a requirement for the overstretching transition at 65 pN.[91] A high ionic strength, by contrast, stabilizes the double helix and inhibits melting-bubble formation. Instead, a different structural form results that cannot be stained by either RPA or Sytox (a dsDNA-intercalating dye). The authors interpreted this form, likely base-paired, as evidence for S-DNA. An increasing ionic strength also suppresses unpeeling and promotes S-DNA formation for topologically open DNA. Thus, the balance between these different processes during overstretching is dependent on DNA sequence, topology, and salt concentration (Figure 4F). An accompanying paper employed magnetic tweezers to study the same transitions and reached essentially the same conclusion.[92] By investigating the temperature effect, the latter study calculated the entropic contribution from each of the three processes. The unpeeling and bubble-melting transitions are hysteretic with a positive entropy change of 17 cal K^{-1} mol^{-1}, similar to thermal melting, whereas the B-to-S transition is nonhysteretic with a small negative entropy change of −2 cal K^{-1} mol^{-1}. Moreover, a recent study adopted concurrent fluorescence polarization imaging and force manipulation to show that base pairs in S-DNA are substantially more tilted than those in B-DNA.[93]

In these types of studies, it is worth keeping in mind the potential perturbation of DNA structure introduced by the intercalating dyes and ssDNA-binding proteins.[94,95] Thus, a low concentration of these reagents is recommended whenever possible. It has also been reported that the fluorescence intensity of intercalating dyes can be used as a sensor for the local tension in dsDNA.[96]

Formation of Nucleoprotein Filaments. Many essential genomic transactions, such as DNA replication, repair, and recombination, involve the generation of ssDNA. Single-molecule studies of these reactions are aided by various experimental strategies to produce long ssDNA templates, such as force-induced duplex melting.[97,98] Using combined fluorescence and force spectroscopy, Ha and co-workers showed that SSB can rapidly diffuse along ssDNA, which facilitates its redistribution.[99] The force dependence of SSB movement suggests that it migrates on DNA via intersegment transfer.[100]

Besides SSB and RPA, there are other proteins that bind to ssDNA, notably RecA for prokaryotes and Rad51 for eukaryotes. These ATPases form nucleoprotein filaments on ssDNA in an ATP-dependent manner and play critical roles in homology search and pairing during homologous recombination.[101] In an earlier study, the Bustamante group interrogated the mechanical properties of RecA−ssDNA and RecA−dsDNA filaments at various nucleotide states.[102] It was found that RecA significantly stiffens and elongates DNA (both RecA−ssDNA and RecA−dsDNA filaments are ~1.5 times longer than bare B-form DNA). Combining fluorescence imaging and flow stretching, the Kowalczykowski group monitored the nucleation and bidirectional growth of RecA−dsDNA filaments[103] and examined the inhibitory effect of SSB on RecA−ssDNA filament assembly.[104] The same group also investigated the process of homology search by RecA−ssDNA filaments on dsDNA.[105] They found that the number of available DNA conformations, which decreases as the end-to-end distance of the target dsDNA is increased, exerts a strong influence on the rate of homologous pairing. Using a dual-molecule manipulation setup combining optical tweezers and magnetic tweezers, the Dekker group also studied the process of homology recognition.[106] By controlling the supercoiling state of the target dsDNA, the authors found that homologous pairing is strongly enhanced by underwinding of the target DNA, which facilitates transient engagement of the incoming duplex by a secondary DNA-binding site in the RecA filament. Both of these studies pointed to a mechanism that harnesses nonspecific and weak interactions between the RecA filament and target dsDNA for a rapid homology search.

Similar to RecA binding, Rad51 binding also extends the DNA by ~50%.[107] The disassembly of Rad51 nucleoprotein filaments occurs at the filament terminus one monomer at a time upon ATP hydrolysis and is sensitive to tension, stalling at forces above 50 pN.[108] By investigating the competition between RPA and Rad51 for DNA binding, Greene and co-workers showed that free RPA in solution inhibits Rad51 filament nucleation, but the elongation of Rad51 filaments on RPA-coated ssDNA is not significantly impacted.[109] Interestingly, it was recently reported that RecA/Rad51 polymerizes faster on S-DNA than on B-DNA,[110] implying potential physiological functions of S-DNA.

■ OUTLOOK

Single-molecule force-manipulation techniques enable precise measurements made at scales highly relevant to the description of DNA mechanics (piconewtons and nanometers). Once its elastic properties were well understood, DNA became an indispensable tool for studying the mechanism of DNA-based biological processes. The integration of fluorescence detection

DOI: 10.1021/acs.biochem.9b00346
Biochemistry 2019, 58, 4667−4676

modality into single-molecule force spectroscopy allows the conformational and mechanical dynamics of DNA or DNA-templated complexes to be simultaneously monitored. These instruments are increasingly becoming commercially available,[111] providing nonspecialists with access to this type of investigation. At the same time, physicists and biophysicists are constantly making technological innovations to further enhance the multiplexity and throughput of single-molecule assays.[112,113] Another critical element for achieving the full power of this type of studies is progress made in the in vitro reconstitution of complex biochemical systems, such as the eukaryotic replisome,[114−116] which allows the function of each component to be unambiguously dissected. Finally, characterization of the physical properties of chromatin and whole chromosomes will contribute to the understanding of genome organization and transcriptional regulation inside the cell.[117] It is anticipated that continued exploration of the mechanical nature of the double helix will lead to a deeper appreciation of how this fundamental molecule orchestrates the operation of living systems.

AUTHOR INFORMATION

Corresponding Author

*E-mail: shixinliu@rockefeller.edu.

ORCID

Shixin Liu: 0000-0003-4238-7066

Funding

M.R.W. is an Anderson Cancer Center Postdoctoral Fellow at the Rockefeller University. S.L. is supported by the Robertson Foundation and the National Institutes of Health (DP2HG010510).

Notes

The authors declare no competing financial interest.

REFERENCES

(1) Watson, J. D., and Crick, F. H. (1953) Molecular structure of nucleic acids; a structure for deoxyribose nucleic acid. *Nature 171*, 737−738.

(2) Wilkins, M. H., Stokes, A. R., and Wilson, H. R. (1953) Molecular structure of deoxypentose nucleic acids. *Nature 171*, 738−740.

(3) Franklin, R. E., and Gosling, R. G. (1953) Molecular configuration in sodium thymonucleate. *Nature 171*, 740−741.

(4) Griffith, J., Huberman, J. A., and Kornberg, A. (1971) Electron microscopy of DNA polymerase bound to DNA. *J. Mol. Biol. 55*, 209−214.

(5) Morikawa, K., and Yanagida, M. (1981) Visualization of individual DNA molecules in solution by light microscopy: DAPI staining method. *J. Biochem. 89*, 693−696.

(6) Houseal, T. W., Bustamante, C., Stump, R. F., and Maestre, M. F. (1989) Real-time imaging of single DNA molecules with fluorescence microscopy. *Biophys. J. 56*, 507−516.

(7) Gurrieri, S., Smith, S. B., Wells, K. S., Johnson, I. D., and Bustamante, C. (1996) Real-time imaging of the reorientation mechanisms of YOYO-labelled DNA molecules during 90 degrees and 120 degrees pulsed field gel electrophoresis. *Nucleic Acids Res 24*, 4759−4767.

(8) Bustamante, C., Bryant, Z., and Smith, S. B. (2003) Ten years of tension: single-molecule DNA mechanics. *Nature 421*, 423−427.

(9) Bryant, Z., Oberstrass, F. C., and Basu, A. (2012) Recent developments in single-molecule DNA mechanics. *Curr. Opin. Struct. Biol. 22*, 304−312.

(10) Ha, T. (2016) Probing Nature's Nanomachines One Molecule at a Time. *Biophys. J. 110*, 1004−1007.

(11) Bustamante, C. (2017) Molecular machines one molecule at a time. *Protein Sci. 26*, 1245−1248.

(12) Neuman, K. C., and Nagy, A. (2008) Single-molecule force spectroscopy: optical tweezers, magnetic tweezers and atomic force microscopy. *Nat. Methods 5*, 491−505.

(13) Smith, S. B., Finzi, L., and Bustamante, C. (1992) Direct mechanical measurements of the elasticity of single DNA molecules by using magnetic beads. *Science 258*, 1122−1126.

(14) Strick, T. R., Allemand, J. F., Bensimon, D., Bensimon, A., and Croquette, V. (1996) The elasticity of a single supercoiled DNA molecule. *Science 271*, 1835−1837.

(15) Cluzel, P., Lebrun, A., Heller, C., Lavery, R., Viovy, J. L., Chatenay, D., and Caron, F. (1996) DNA: an extensible molecule. *Science 271*, 792−794.

(16) Perkins, T. T., Smith, D. E., Larson, R. G., and Chu, S. (1995) Stretching of a single tethered polymer in a uniform flow. *Science 268*, 83−87.

(17) Smith, S. B., Cui, Y., and Bustamante, C. (1996) Overstretching B-DNA: the elastic response of individual double-stranded and single-stranded DNA molecules. *Science 271*, 795−799.

(18) Bustamante, C., Marko, J. F., Siggia, E. D., and Smith, S. (1994) Entropic elasticity of lambda-phage DNA. *Science 265*, 1599−1600.

(19) Wang, M. D., Yin, H., Landick, R., Gelles, J., and Block, S. M. (1997) Stretching DNA with optical tweezers. *Biophys. J. 72*, 1335−1346.

(20) Baumann, C. G., Smith, S. B., Bloomfield, V. A., and Bustamante, C. (1997) Ionic effects on the elasticity of single DNA molecules. *Proc. Natl. Acad. Sci. U. S. A. 94*, 6185−6190.

(21) Vafabakhsh, R., and Ha, T. (2012) Extreme bendability of DNA less than 100 base pairs long revealed by single-molecule cyclization. *Science 337*, 1097−1101.

(22) Yan, J., and Marko, J. F. (2004) Localized single-stranded bubble mechanism for cyclization of short double helix DNA. *Phys. Rev. Lett. 93*, 108108.

(23) Wiggins, P. A., Phillips, R., and Nelson, P. C. (2005) Exact theory of kinkable elastic polymers. *Phys. Rev. E Stat. Nonlin. Soft Matter Phys. 71*, 021909.

(24) Gross, P., Laurens, N., Oddershede, L. B., Bockelmann, U., Peterman, E. J., and Wuite, G. J. (2011) Quantifying how DNA stretches, melts and changes twist under tension. *Nat. Phys. 7*, 731−736.

(25) Strick, T. R., Allemand, J. F., Bensimon, D., and Croquette, V. (1998) Behavior of supercoiled DNA. *Biophys. J. 74*, 2016−2028.

(26) Gore, J., Bryant, Z., Nollmann, M., Le, M. U., Cozzarelli, N. R., and Bustamante, C. (2006) DNA overwinds when stretched. *Nature 442*, 836−839.

(27) Heller, I., Hoekstra, T. P., King, G. A., Peterman, E. J., and Wuite, G. J. (2014) Optical tweezers analysis of DNA-protein complexes. *Chem. Rev. 114*, 3087−3119.

(28) Wuite, G. J., Smith, S. B., Young, M., Keller, D., and Bustamante, C. (2000) Single-molecule studies of the effect of template tension on T7 DNA polymerase activity. *Nature 404*, 103−106.

(29) Sarkar, A., Leger, J. F., Chatenay, D., and Marko, J. F. (2001) Structural transitions in DNA driven by external force and torque. *Phys. Rev. E Stat. Nonlin. Soft Matter Phys. 63*, 051903.

(30) Camunas-Soler, J., Ribezzi-Crivellari, M., and Ritort, F. (2016) Elastic Properties of Nucleic Acids by Single-Molecule Force Spectroscopy. *Annu. Rev. Biophys. 45*, 65−84.

(31) Calladine, C. R., Drew, H. R., Luisi, B. F., and Travers, A. A. (2004) *Understanding DNA: The molecule and how it works*, Elsevier Academic Press.

(32) Williams, M. C., Rouzina, I., and Bloomfield, V. A. (2002) Thermodynamics of DNA interactions from single molecule stretching experiments. *Acc. Chem. Res. 35*, 159−166.

(33) van Mameren, J., Gross, P., Farge, G., Hooijman, P., Modesti, M., Falkenberg, M., Wuite, G. J., and Peterman, E. J. (2009) Unraveling the structure of DNA during overstretching by using

DOI: 10.1021/acs.biochem.9b00346
Biochemistry 2019, 58, 4667−4676

multicolor, single-molecule fluorescence imaging. *Proc. Natl. Acad. Sci. U. S. A. 106*, 18231−18236.
(34) Fu, H., Chen, H., Marko, J. F., and Yan, J. (2010) Two distinct overstretched DNA states. *Nucleic Acids Res. 38*, 5594−5600.
(35) Bosaeus, N., El-Sagheer, A. H., Brown, T., Smith, S. B., Akerman, B., Bustamante, C., and Norden, B. (2012) Tension induces a base-paired overstretched DNA conformation. *Proc. Natl. Acad. Sci. U. S. A. 109*, 15179−15184.
(36) Allemand, J. F., Bensimon, D., Lavery, R., and Croquette, V. (1998) Stretched and overwound DNA forms a Pauling-like structure with exposed bases. *Proc. Natl. Acad. Sci. U. S. A. 95*, 14152−14157.
(37) King, G. A., Peterman, E. J., and Wuite, G. J. (2016) Unravelling the structural plasticity of stretched DNA under torsional constraint. *Nat. Commun. 7*, 11810.
(38) Forth, S., Sheinin, M. Y., Inman, J., and Wang, M. D. (2013) Torque measurement at the single-molecule level. *Annu. Rev. Biophys. 42*, 583−604.
(39) Lipfert, J., van Oene, M. M., Lee, M., Pedaci, F., and Dekker, N. H. (2015) Torque spectroscopy for the study of rotary motion in biological systems. *Chem. Rev. 115*, 1449−1474.
(40) Sheinin, M. Y., Forth, S., Marko, J. F., and Wang, M. D. (2011) Underwound DNA under tension: structure, elasticity, and sequence-dependent behaviors. *Phys. Rev. Lett. 107*, 108102.
(41) Hao, Y., Canavan, C., Taylor, S. S., and Maillard, R. A. (2017) Integrated Method to Attach DNA Handles and Functionally Select Proteins to Study Folding and Protein-Ligand Interactions with Optical Tweezers. *Sci. Rep. 7*, 10843.
(42) Liphardt, J., Onoa, B., Smith, S. B., Tinoco, I., Jr., and Bustamante, C. (2001) Reversible unfolding of single RNA molecules by mechanical force. *Science 292*, 733−737.
(43) Liu, K., Maciuba, K., and Kaiser, C. M. (2019) The Ribosome Cooperates with a Chaperone to Guide Multi-domain Protein Folding. *Mol. Cell 74*, 310−319.
(44) Zananiri, R., Malik, O., Rudnizky, S., Gaydar, V., Kreiserman, R., Henn, A., and Kaplan, A. (2019) Synergy between RecBCD subunits is essential for efficient DNA unwinding. *eLife 8*, No. e40836.
(45) Pfitzner, E., Wachauf, C., Kilchherr, F., Pelz, B., Shih, W. M., Rief, M., and Dietz, H. (2013) Rigid DNA beams for high-resolution single-molecule mechanics. *Angew. Chem. Int. Ed. 52*, 7766−7771.
(46) Kilchherr, F., Wachauf, C., Pelz, B., Rief, M., Zacharias, M., and Dietz, H. (2016) Single-molecule dissection of stacking forces in DNA. *Science 353*, No. aaf5508.
(47) Hall, M. A., Shundrovsky, A., Bai, L., Fulbright, R. M., Lis, J. T., and Wang, M. D. (2009) High-resolution dynamic mapping of histone-DNA interactions in a nucleosome. *Nat. Struct. Mol. Biol. 16*, 124−129.
(48) Burnham, D. R., Kose, H. B., Hoyle, R. B., and Yardimci, H. (2019) The mechanism of DNA unwinding by the eukaryotic replicative helicase. *Nat. Commun. 10*, 2159.
(49) Ma, J., Bai, L., and Wang, M. D. (2013) Transcription under torsion. *Science 340*, 1580−1583.
(50) Stone, M. D., Bryant, Z., Crisona, N. J., Smith, S. B., Vologodskii, A., Bustamante, C., and Cozzarelli, N. R. (2003) Chirality sensing by Escherichia coli topoisomerase IV and the mechanism of type II topoisomerases. *Proc. Natl. Acad. Sci. U. S. A. 100*, 8654−8659.
(51) Bustamante, C., Cheng, W., and Mejia, Y. X. (2011) Revisiting the central dogma one molecule at a time. *Cell 144*, 480−497.
(52) Abbondanzieri, E. A., Greenleaf, W. J., Shaevitz, J. W., Landick, R., and Block, S. M. (2005) Direct observation of base-pair stepping by RNA polymerase. *Nature 438*, 460−465.
(53) Moffitt, J. R., Chemla, Y. R., Aathavan, K., Grimes, S., Jardine, P. J., Anderson, D. L., and Bustamante, C. (2009) Intersubunit coordination in a homomeric ring ATPase. *Nature 457*, 446−450.
(54) Mao, H., Saha, M., Reyes-Aldrete, E., Sherman, M. B., Woodson, M., Atz, R., Grimes, S., Jardine, P. J., and Morais, M. C. (2016) Structural and Molecular Basis for Coordination in a Viral DNA Packaging Motor. *Cell Rep. 14*, 2017−2029.
(55) Chemla, Y. R., Aathavan, K., Michaelis, J., Grimes, S., Jardine, P. J., Anderson, D. L., and Bustamante, C. (2005) Mechanism of force generation of a viral DNA packaging motor. *Cell 122*, 683−692.
(56) Chistol, G., Liu, S., Hetherington, C. L., Moffitt, J. R., Grimes, S., Jardine, P. J., and Bustamante, C. (2012) High degree of coordination and division of labor among subunits in a homomeric ring ATPase. *Cell 151*, 1017−1028.
(57) Tafoya, S., Liu, S., Castillo, J. P., Atz, R., Morais, M. C., Grimes, S., Jardine, P. J., and Bustamante, C. (2018) Molecular switch-like regulation enables global subunit coordination in a viral ring ATPase. *Proc. Natl. Acad. Sci. U. S. A. 115*, 7961−7966.
(58) Liu, S., Chistol, G., Hetherington, C. L., Tafoya, S., Aathavan, K., Schnitzbauer, J., Grimes, S., Jardine, P. J., and Bustamante, C. (2014) A viral packaging motor varies its DNA rotation and step size to preserve subunit coordination as the capsid fills. *Cell 157*, 702−713.
(59) Aathavan, K., Politzer, A. T., Kaplan, A., Moffitt, J. R., Chemla, Y. R., Grimes, S., Jardine, P. J., Anderson, D. L., and Bustamante, C. (2009) Substrate interactions and promiscuity in a viral DNA packaging motor. *Nature 461*, 669−673.
(60) Hendrix, R. W. (1978) Symmetry mismatch and DNA packaging in large bacteriophages. *Proc. Natl. Acad. Sci. U. S. A. 75*, 4779−4783.
(61) Xu, J., Wang, D., Gui, M., and Xiang, Y. (2019) Structural assembly of the tailed bacteriophage ϕ29. *Nat. Commun. 10*, 2366.
(62) Bryant, Z., Stone, M. D., Gore, J., Smith, S. B., Cozzarelli, N. R., and Bustamante, C. (2003) Structural transitions and elasticity from torque measurements on DNA. *Nature 424*, 338−341.
(63) Smith, D. E., Tans, S. J., Smith, S. B., Grimes, S., Anderson, D. L., and Bustamante, C. (2001) The bacteriophage straight phi29 portal motor can package DNA against a large internal force. *Nature 413*, 748−752.
(64) Kindt, J., Tzlil, S., Ben-Shaul, A., and Gelbart, W. M. (2001) DNA packaging and ejection forces in bacteriophage. *Proc. Natl. Acad. Sci. U. S. A. 98*, 13671−13674.
(65) Purohit, P. K., Inamdar, M. M., Grayson, P. D., Squires, T. M., Kondev, J., and Phillips, R. (2005) Forces during bacteriophage DNA packaging and ejection. *Biophys. J. 88*, 851−866.
(66) Spakowitz, A. J., and Wang, Z. G. (2005) DNA packaging in bacteriophage: is twist important? *Biophys. J. 88*, 3912−3923.
(67) Sharp, K. A., Lu, X.-J., Cingolani, G., and Harvey, S. C. (2019) DNA conformational changes play a force-generating role during bacteriophage genome packaging. *Biophys. J. 116*, 2172−2180.
(68) Maier, B., Bensimon, D., and Croquette, V. (2000) Replication by a single DNA polymerase of a stretched single-stranded DNA. *Proc. Natl. Acad. Sci. U. S. A. 97*, 12002−12007.
(69) Ibarra, B., Chemla, Y. R., Plyasunov, S., Smith, S. B., Lazaro, J. M., Salas, M., and Bustamante, C. (2009) Proofreading dynamics of a processive DNA polymerase. *EMBO J. 28*, 2794−2802.
(70) van Oijen, A. M., Blainey, P. C., Crampton, D. J., Richardson, C. C., Ellenberger, T., and Xie, X. S. (2003) Single-molecule kinetics of lambda exonuclease reveal base dependence and dynamic disorder. *Science 301*, 1235−1238.
(71) Lee, J. B., Hite, R. K., Hamdan, S. M., Xie, X. S., Richardson, C. C., and van Oijen, A. M. (2006) DNA primase acts as a molecular brake in DNA replication. *Nature 439*, 621−624.
(72) Pandey, M., Syed, S., Donmez, I., Patel, G., Ha, T., and Patel, S. S. (2009) Coordinating DNA replication by means of priming loop and differential synthesis rate. *Nature 462*, 940−943.
(73) Manosas, M., Spiering, M. M., Zhuang, Z., Benkovic, S. J., and Croquette, V. (2009) Coupling DNA unwinding activity with primer synthesis in the bacteriophage T4 primosome. *Nat. Chem. Biol. 5*, 904−912.
(74) Hamdan, S. M., Loparo, J. J., Takahashi, M., Richardson, C. C., and van Oijen, A. M. (2009) Dynamics of DNA replication loops reveal temporal control of lagging-strand synthesis. *Nature 457*, 336−339.
(75) Lewis, J. S., Spenkelink, L. M., Schauer, G. D., Hill, F. R., Georgescu, R. E., O'Donnell, M. E., and van Oijen, A. M. (2017) Single-molecule visualization of Saccharomyces cerevisiae leading-

DOI: 10.1021/acs.biochem.9b00346
Biochemistry 2019, 58, 4667−4676

strand synthesis reveals dynamic interaction between MTC and the replisome. *Proc. Natl. Acad. Sci. U. S. A. 114*, 10630−10635.
(76) van Oijen, A. M. (2007) Honey, I shrunk the DNA: DNA length as a probe for nucleic-acid enzyme activity. *Biopolymers 85*, 144−153.
(77) Duderstadt, K. E., Geertsema, H. J., Stratmann, S. A., Punter, C. M., Kulczyk, A. W., Richardson, C. C., and van Oijen, A. M. (2016) Simultaneous Real-Time Imaging of Leading and Lagging Strand Synthesis Reveals the Coordination Dynamics of Single Replisomes. *Mol. Cell 64*, 1035−1047.
(78) Tanner, N. A., Hamdan, S. M., Jergic, S., Loscha, K. V., Schaeffer, P. M., Dixon, N. E., and van Oijen, A. M. (2008) Single-molecule studies of fork dynamics in Escherichia coli DNA replication. *Nat. Struct. Mol. Biol. 15*, 170−176.
(79) Loparo, J. J., Kulczyk, A. W., Richardson, C. C., and van Oijen, A. M. (2011) Simultaneous single-molecule measurements of phage T7 replisome composition and function reveal the mechanism of polymerase exchange. *Proc. Natl. Acad. Sci. U. S. A. 108*, 3584−3589.
(80) Duzdevich, D., Warner, M. D., Ticau, S., Ivica, N. A., Bell, S. P., and Greene, E. C. (2015) The dynamics of eukaryotic replication initiation: origin specificity, licensing, and firing at the single-molecule level. *Mol. Cell 58*, 483−494.
(81) Graham, J. E., Marians, K. J., and Kowalczykowski, S. C. (2017) Independent and Stochastic Action of DNA Polymerases in the Replisome. *Cell 169*, 1201−1213.
(82) Sparks, J. L., Chistol, G., Gao, A. O., Raschle, M., Larsen, N. B., Mann, M., Duxin, J. P., and Walter, J. C. (2019) The CMG Helicase Bypasses DNA-Protein Cross-Links to Facilitate Their Repair. *Cell 176*, 167−181.
(83) Harada, Y., Funatsu, T., Murakami, K., Nonoyama, Y., Ishihama, A., and Yanagida, T. (1999) Single-molecule imaging of RNA polymerase-DNA interactions in real time. *Biophys. J. 76*, 709−715.
(84) Lang, M. J., Fordyce, P. M., and Block, S. M. (2003) Combined optical trapping and single-molecule fluorescence. *J. Biol. 2*, 6.
(85) Candelli, A., Wuite, G. J., and Peterman, E. J. (2011) Combining optical trapping, fluorescence microscopy and micro-fluidics for single molecule studies of DNA-protein interactions. *Phys. Chem. Chem. Phys. 13*, 7263−7272.
(86) Comstock, M. J., Ha, T., and Chemla, Y. R. (2011) Ultrahigh-resolution optical trap with single-fluorophore sensitivity. *Nat. Methods 8*, 335−340.
(87) Graves, E. T., Duboc, C., Fan, J., Stransky, F., Leroux-Coyau, M., and Strick, T. R. (2015) A dynamic DNA-repair complex observed by correlative single-molecule nanomanipulation and fluorescence. *Nat. Struct. Mol. Biol. 22*, 452−457.
(88) Suksombat, S., Khafizov, R., Kozlov, A. G., Lohman, T. M., and Chemla, Y. R. (2015) Structural dynamics of E. coli single-stranded DNA binding protein reveal DNA wrapping and unwrapping pathways. *eLife 4*, No. e08193.
(89) Leger, J. F., Romano, G., Sarkar, A., Robert, J., Bourdieu, L., Chatenay, D., and Marko, J. F. (1999) Structural transitions of a twisted and stretched DNA molecule. *Phys. Rev. Lett. 83*, 1066−1069.
(90) King, G. A., Gross, P., Bockelmann, U., Modesti, M., Wuite, G. J., and Peterman, E. J. (2013) Revealing the competition between peeled ssDNA, melting bubbles, and S-DNA during DNA over-stretching using fluorescence microscopy. *Proc. Natl. Acad. Sci. U. S. A. 110*, 3859−3864.
(91) Paik, D. H., and Perkins, T. T. (2011) Overstretching DNA at 65 pN does not require peeling from free ends or nicks. *J. Am. Chem. Soc. 133*, 3219−3221.
(92) Zhang, X., Chen, H., Le, S., Rouzina, I., Doyle, P. S., and Yan, J. (2013) Revealing the competition between peeled ssDNA, melting bubbles, and S-DNA during DNA overstretching by single-molecule calorimetry. *Proc. Natl. Acad. Sci. U. S. A. 110*, 3865−3870.
(93) Backer, A. S., Biebricher, A. S., King, G. A., Wuite, G. J. L., Heller, I., and Peterman, E. J. G. (2019) Single-molecule polarization microscopy of DNA intercalators sheds light on the structure of S-DNA. *Sci. Adv. 5*, No. eaav1083.
(94) Shokri, L., Rouzina, I., and Williams, M. C. (2009) Interaction of bacteriophage T4 and T7 single-stranded DNA-binding proteins with DNA. *Phys. Biol. 6*, 025002.
(95) Biebricher, A. S., Heller, I., Roijmans, R. F., Hoekstra, T. P., Peterman, E. J., and Wuite, G. J. (2015) The impact of DNA intercalators on DNA and DNA-processing enzymes elucidated through force-dependent binding kinetics. *Nat. Commun. 6*, 7304.
(96) King, G. A., Biebricher, A. S., Heller, I., Peterman, E. J. G., and Wuite, G. J. L. (2018) Quantifying Local Molecular Tension Using Intercalated DNA Fluorescence. *Nano Lett. 18*, 2274−2281.
(97) Candelli, A., Hoekstra, T. P., Farge, G., Gross, P., Peterman, E. J., and Wuite, G. J. (2013) A toolbox for generating single-stranded DNA in optical tweezers experiments. *Biopolymers 99*, 611−620.
(98) Lee, K. S., Balci, H., Jia, H., Lohman, T. M., and Ha, T. (2013) Direct imaging of single UvrD helicase dynamics on long single-stranded DNA. *Nat. Commun. 4*, 1878.
(99) Zhou, R., Kozlov, A. G., Roy, R., Zhang, J., Korolev, S., Lohman, T. M., and Ha, T. (2011) SSB functions as a sliding platform that migrates on DNA via reptation. *Cell 146*, 222−232.
(100) Lee, K. S., Marciel, A. B., Kozlov, A. G., Schroeder, C. M., Lohman, T. M., and Ha, T. (2014) Ultrafast redistribution of E. coli SSB along long single-stranded DNA via intersegment transfer. *J. Mol. Biol. 426*, 2413−2421.
(101) Bell, J. C., and Kowalczykowski, S. C. (2016) Mechanics and Single-Molecule Interrogation of DNA Recombination. *Annu. Rev. Biochem. 85*, 193−226.
(102) Hegner, M., Smith, S. B., and Bustamante, C. (1999) Polymerization and mechanical properties of single RecA-DNA filaments. *Proc. Natl. Acad. Sci. U. S. A. 96*, 10109−10114.
(103) Galletto, R., Amitani, I., Baskin, R. J., and Kowalczykowski, S. C. (2006) Direct observation of individual RecA filaments assembling on single DNA molecules. *Nature 443*, 875−878.
(104) Bell, J. C., Plank, J. L., Dombrowski, C. C., and Kowalczykowski, S. C. (2012) Direct imaging of RecA nucleation and growth on single molecules of SSB-coated ssDNA. *Nature 491*, 274−278.
(105) Forget, A. L., and Kowalczykowski, S. C. (2012) Single-molecule imaging of DNA pairing by RecA reveals a three-dimensional homology search. *Nature 482*, 423−427.
(106) De Vlaminck, I., van Loenhout, M. T., Zweifel, L., den Blanken, J., Hooning, K., Hage, S., Kerssemakers, J., and Dekker, C. (2012) Mechanism of homology recognition in DNA recombination from dual-molecule experiments. *Mol. Cell 46*, 616−624.
(107) Hilario, J., Amitani, I., Baskin, R. J., and Kowalczykowski, S. C. (2009) Direct imaging of human Rad51 nucleoprotein dynamics on individual DNA molecules. *Proc. Natl. Acad. Sci. U. S. A. 106*, 361−368.
(108) van Mameren, J., Modesti, M., Kanaar, R., Wyman, C., Peterman, E. J., and Wuite, G. J. (2009) Counting RAD51 proteins disassembling from nucleoprotein filaments under tension. *Nature 457*, 745−748.
(109) Ma, C. J., Gibb, B., Kwon, Y., Sung, P., and Greene, E. C. (2017) Protein dynamics of human RPA and RAD51 on ssDNA during assembly and disassembly of the RAD51 filament. *Nucleic Acids Res. 45*, 749−761.
(110) Zhao, X. C., Fu, H., Song, L., Yang, Y. J., Zhou, E. C., Liu, G. X., Chen, X. F., Li, Z., Wu, W. Q., and Zhang, X. H. (2019) S-DNA and RecA/RAD51-Mediated Strand Exchange in Vitro. *Biochemistry 58*, 2009−2016.
(111) van Mameren, J., Wuite, G. J. L., and Heller, I. (2018) Introduction to Optical Tweezers: Background, System Designs, and Commercial Solutions. *Methods Mol. Biol. 1665*, 3−23.
(112) Brouwer, I., Sitters, G., Candelli, A., Heerema, S. J., Heller, I., de Melo, A. J., Zhang, H., Normanno, D., Modesti, M., Peterman, E. J., and Wuite, G. J. (2016) Sliding sleeves of XRCC4-XLF bridge DNA and connect fragments of broken DNA. *Nature 535*, 566−569.
(113) Nathwani, B., Shih, W. M., and Wong, W. P. (2018) Force Spectroscopy and Beyond: Innovations and Opportunities. *Biophys. J. 115*, 2279−2285.

DOI: 10.1021/acs.biochem.9b00346
Biochemistry 2019, 58, 4667−4676

(114) Georgescu, R. E., Schauer, G. D., Yao, N. Y., Langston, L. D., Yurieva, O., Zhang, D., Finkelstein, J., and O'Donnell, M. E. (2015) Reconstitution of a eukaryotic replisome reveals suppression mechanisms that define leading/lagging strand operation. *eLife 4*, No. e04988.
(115) Yeeles, J. T., Deegan, T. D., Janska, A., Early, A., and Diffley, J. F. (2015) Regulated eukaryotic DNA replication origin firing with purified proteins. *Nature 519*, 431−435.
(116) Wasserman, M. R., Schauer, G. D., O'Donnell, M. E., and Liu, S. (2019) Replication Fork Activation Is Enabled by a Single-stranded DNA Gate in CMG Helicase. *Cell*, in press.
(117) Stephens, A. D., Banigan, E. J., and Marko, J. F. (2019) Chromatin's physical properties shape the nucleus and its functions. *Curr. Opin. Cell Biol. 58*, 76−84.

DOI: 10.1021/acs.biochem.9b00346
Biochemistry 2019, 58, 4667−4676